**Atmospheric
Chemistry
and Physics
Discussions**

Hydroxyl radical reactivity at the air-ice interface

T. F. Kahan[1], R. Zhao[1], and D. J. Donaldson[1,2]

[1]Department of Chemistry, University of Toronto, 80 Saint George Street, Toronto, M5S 3H6 Ontario, Canada
[2]Department of Physical and Environmental Sciences, University of Toronto at Scarborough, Toronto, M1C 1A4 Ontario, Canada

Correspondence to: D. J. Donaldson (jdonalds@chem.utoronto.ca)

Title Page

Abstract	Introduction
Conclusions	References
Tables	Figures

|◄|►|
|◄|►|

| Back | Close |

Full Screen / Esc

Printer-friendly Version

Interactive Discussion

Abstract

Hydroxyl radicals are important oxidants in the atmosphere and in natural waters. They are also expected to be important in snow and ice, but their reactivity has not been widely studied in frozen aqueous solution. We have developed a spectroscopic probe to monitor the formation and reactions of hydroxyl radicals in situ. Hydroxyl radicals are produced in aqueous solution via the photolysis of nitrite, nitrate, and hydrogen peroxide, and react rapidly with benzene to form phenol. Similar phenol formation rates were observed in aqueous solution and bulk ice. However, no reaction was observed at the air-ice interface, or when bulk ice samples were crushed prior to photolysis to increase their surface area. We also monitored the heterogeneous reaction between benzene present at air-water and air-ice interfaces with gas-phase OH produced from HONO photolysis. Rapid phenol formation was observed on water surfaces, but no reaction was observed at the surface of ice. Under the same conditions, we observed rapid loss of the polycyclic aromatic hydrocarbon (PAH) anthracene at the air-water interface, but no loss was observed at the air-ice interface. Our results suggest that the reactivity of hydroxyl radicals toward aromatic organics is similar in bulk ice samples and in aqueous solution, but is significantly suppressed in the quasi-liquid layer (QLL) that exists at the air-ice interface.

1 Introduction

Reactions involving hydroxyl radicals are of great interest in environmental chemistry. Hydroxyl radicals react readily with organic pollutants in the atmosphere and in natural waters; it is expected that the same is true in snow and ice (e.g. Anastasio et al., 2007). If they occur, such reactions would be important both in snow-covered urban centres, where organic pollutants are ubiquitous, and also in remote polar regions, where organic pollutants such as polycyclic aromatic hydrocarbons (PAHs) have been detected in snow and ice (Schrimpff et al., 1979; Jaffrezo et al., 1994; Franz and Eisenreich,

2000; Masclet et al., 2000; Carrera et al., 2001; Compoint et al., 2002; Slater et al., 2002; Fernandez et al., 2003; Melnikov et al., 2003; Cincinelli et al., 2005; Daly and Wania 2005; Herbert et al., 2006; Wang et al., 2008; Wang et al., 2008). Hydroxyl radical mixing ratios in the air above polar snowpacks can be as high as those in urban centres, due primarily to photochemical production within the snowpack. (See Domine and Shepson, 2002; Grannas et al., 2007 for a discussion of the state of knowledge on organics in snow packs.)

Snow and ice are important substrates for a range of atmospherically relevant reactions (Domine and Shepson 2002; Grannas et al., 2007). A number of studies have investigated the photolysis of inorganic (Dubowski et al., 2001; Dubowski et al., 2002; Qiu et al., 2002; Chu and Anastasio 2003; Cotter et al., 2003; Chu and Anastasio 2005; Jacobi et al., 2006; Anastasio et al., 2007; Chu and Anastasio 2007; Anastasio and Chu 2009) and organic (Dubowski and Hoffmann 2000; Klan and Holoubek 2002; Klan et al., 2003; Klanova et al., 2003; Klanova et al., 2003; Grannas et al., 2007; Kahan and Donaldson 2007; Ram and Anastasio 2009) compounds in these media under conditions relevant to Earth's surface, and a handful (Klanova et al., 2003; Grannas et al., 2007; Kahan and Donaldson, 2007, 2008; Matykiewiczova et al., 2007; Ram and Anastasio, 2009) have examined bimolecular reactions. Some studies (Chu and Anastasio, 2003; Cotter et al., 2003; Chu and Anastasio, 2005; Jacobi et al., 2006; Chu and Anastasio, 2007; Anastasio and Chu, 2009; Ram and Anastasio, 2009) indicate that reaction kinetics are similar in ice and in aqueous solution, while others (Dubowski and Hoffmann, 2000; Klanova et al., 2003; Grannas et al., 2007; Kahan and Donaldson, 2007, 2008) suggest that reactivity is different in the two media. Although treating ice as a similar reaction medium to liquid water makes modelling the chemical fate of species in ice straightforward, laboratory results do not necessarily support this approach. While similar reaction rates for OH with the PAHs phenanthrene, pyrene, and fluoranthene have been reported in water and ice (Ram and Anastasio, 2009), degradation of monochlorophenols in the presence of hydroxyl radicals is reported to occur more slowly in ice compared to in aqueous solution (Klanova et al., 2003), and

anthracene was not observed to react with OH at the air-ice interface (Kahan and Donaldson, 2007).

Some of the contradictions in the above-mentioned laboratory results could be due to the heterogeneity of ice in laboratory-prepared samples and in the natural environment. Specifically, it may be that the reactivity of PAHs is different in the two parts of ice where reactions are most likely to occur: Liquid pockets within bulk ice, and in the disordered region at the air-ice interface referred to as the quasi-liquid layer (QLL). (For a discussion of the physical properties of ice as they relate to snowpack photochemistry, see Domine et al., 2008).

The idea that the bulk and the surface of ice present two distinct reaction environments is based on the observation that the photolysis rates of anthracene and naphthalene (Kahan and Donaldson, 2007) measured in situ at the air-ice interface were greatly enhanced compared to the rates in solution, whereas the photolysis rates of phenanthrene, pyrene, and fluoranthene (Ram and Anastasio, 2009) measured by analyzing melted ice samples were not. To test this hypothesis, we measured (Kahan et al., 2009) photolysis kinetics of anthracene solutions frozen into large ice cubes, as well as the kinetics when the ice cubes were crushed to yield higher surface area-to-volume ratios under identical illumination. Photolysis proceeded at a similar rate in the ice cubes as in room temperature aqueous solution, but the rate in the crushed ice was approximately five times faster (Kahan et al., 2009). This enhanced rate matched that measured previously (Kahan and Donaldson, 2007) directly at the air-ice interface using the same illumination system.

The results described above confirm that photoreactivity in the QLL can be different from that in liquid pockets present within bulk ice. In this work we test a hypothesis that the reactivity of OH toward organic compounds is also different in these two locations. If the production rate or reactivity of OH is suppressed at the air-ice interface compared to in bulk ice, the discrepancy in indirect photolysis rates of PAHs measured in the QLL (Kahan and Donaldson, 2007) and in bulk ice (Ram and Anastasio, 2009) could be resolved. To explore this possibility, here we irradiated aqueous benzene solutions

containing the photochemical OH precursors NO_2^-, NO_3^-, and H_2O_2, and compared phenol formation kinetics in aqueous solution, ice cubes, and crushed ice to determine the effect of the reagents' location in ice on the observed reaction kinetics. We further performed real-time measurements of the same reactions in situ in solution and in the QLL, and also monitored the heterogeneous reactions between OH(g) and benzene or anthracene at the air-ice interface. Together, the results show that while the reactivity of hydroxyl radicals toward aromatic species is similar in bulk ice to that measured in, or at the surface of, aqueous solution, it is significantly suppressed at the air-ice interface.

2 Methods

2.1 Overview

In this study, we explored the formation of OH. While benzene has been used as a trap to measure OH formation rates in natural waters (e.g. Vione et al., 2006), and in acetonitrile-water mixtures at temperatures below 0°C (Galbavy et al., 2007), it has not previously been used as an in situ, real time probe. It has also, to our knowledge, never been used in frozen samples.

Several types of experiments were performed: (a) Offline measurements of phenol formed from the reaction of benzene with photoformed OH; (b) development of an in situ probe to measure OH reactivity via reaction with benzene; (c) use of this probe to monitor OH in aqueous solution; (d) extension of the measurements to the air-ice interface; and (e) in situ measurements of reactions between gas-phase OH and aromatics at liquid or solid aqueous interfaces.

In (a), aqueous samples containing benzene and H_2O_2 were frozen. Ice samples with varying surface area-to-volume ratios were irradiated and the phenol formation rates were contrasted with those in aqueous solution under the same conditions. In (b), we developed and validated a technique to measure phenol formation rates in situ in aqueous solution and at the air-ice interface using laser-induced fluorescence (LIF). In

(c) we used the in situ technique to measure phenol formation rates in aqueous solution due to the photolysis of H_2O_2, NO_3^-, and NO_2^- in aqueous solution. We used our results to calculate the photon flux of our lamp, which was compared to the predicted flux to further validate the in situ technique. In (d) we monitored phenol formation at the air-ice interface due to the photolysis of the hydroxyl radical precursors, and in (e) we formed OH in the gas phase through HONO photolysis, and monitored its reaction with benzene or anthracene present at air-water and air-ice interfaces.

2.2 Offline measurements: experiment set (a)

2.2.1 Sample preparation

Aqueous solutions containing 1.1×10^{-3} mol L^{-1} benzene and 9.9×10^{-4} mol L^{-1} H_2O_2 were prepared daily. Ice cubes were prepared (Kahan et al., 2009) by freezing 3 to 5 mL aliquots of aqueous solutions into semi-spheres with radii of ~1 cm in an ice cube tray. Ice granules with radii of ~2 mm were prepared by crushing the ice cubes. The samples were crushed on the chilled floor of the reaction chamber described below to prevent melting.

2.2.2 Experimental details

Samples were irradiated by the output of a 75 W xenon arc lamp which passed through a 295 nm longpass cutoff filter. Aqueous samples were irradiated at room temperature in 10 mm pathlength quartz cuvettes. The lamp was situated approximately 50 cm from the sample, and the beam was centered on the cuvette. Solutions were irradiated for up to two hours. At known time intervals, the samples were removed from the light and excitation spectra were acquired using a commercial fluorimeter. Excitation and emission wavelengths for all spectra are detailed in Table 1.

Ice cubes and ice granules were placed on a stainless steel plate in the center of a reaction chamber consisting of a stainless steel chamber with a copper floor under

which copper cooling tubes passed. The temperature inside the chamber was maintained at approximately −16°C. The lamp's output was directed by a first-surface mirror with maximum reflectance at 355 nm into the chamber through an opening in the roof so that the sample was evenly illuminated. The distance between the lamp and the sample was approximately 75 cm. Samples were irradiated for a known time period, then melted into brown glass bottles and stored in the dark until analysis. Excitation spectra were acquired in quartz cuvettes. Analysis was always performed on the same day as photolysis.

Reaction kinetics between benzene and OH were obtained by measuring the growth rate of phenol during photolysis. Figure 1 shows excitation and emission spectra of benzene and phenol in aqueous solution. The emission spectra of the two species overlap almost entirely, but phenol absorbs at wavelengths above 270 nm, whereas benzene does not. To minimize interferences from benzene, we monitored the growth of phenol intensity using 271 nm as the excitation wavelength and 318 nm for emission, as indicated by the arrows in the figure. Excitation spectra were acquired at a scan rate of 100 nm min^{-1} and with slit widths of 4.5 nm. Emission intensity was related to phenol concentration using a Beer-Lambert plot, as described in the supplementary information http://www.atmos-chem-phys-discuss.net/9/20881/2009/acpd-9-20881-2009-supplement.pdf.

2.3 In situ measurements: experiment sets (b)–(e)

2.3.1 Sample preparation

For the experiments in (b), aqueous solutions containing 10^{-6} to 10^{-3} mol L^{-1} benzene were prepared daily. Ice samples for the in situ QLL measurements were prepared as described previously (Kahan and Donaldson, 2007). Approximately 1 mL of aqueous solution was frozen on a stainless steel plate in a Teflon chamber (Kahan and Donaldson, 2007) with a copper floor under which copper cooling tubes run. Ports in the walls allow gas-phase species to be introduced and vented. After freezing, the ice was

inverted to present a flat surface to the laser. The temperature within the chamber was maintained at approximately $-16°C$. To ensure that benzene was present at the air-ice interface, some ice samples were prepared by freezing pure water and then depositing benzene to the ice surface from the gas phase by sampling the headspace above liquid

5   benzene using a Pasteur pipette, and "puffing" it onto the ice surface.

For (c), aqueous solutions containing $1.2\times10^{-3}\,mol\,L^{-1}$ benzene and 10^{-5} to $10^{-3}\,mol\,L^{-1}$ $NaNO_2$, H_2O_2, or HNO_3 as OH precursors were prepared daily. Ice samples for (d) were prepared as in (b), with benzene concentrations ranging from 10^{-6} to $10^{-3}\,mol\,L^{-1}$, and OH-precursor concentrations ranging from 10^{-5} to $10^{-3}\,mol\,L^{-1}$.

10 For some experiments, both benzene and nitric acid were introduced to the ice surface from the gas phase. Nitric acid was introduced in a similar fashion as benzene, by sampling the headspace above a concentrated HNO_3 solution (Kahan and Donaldson, 2007).
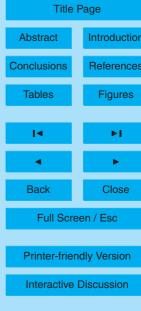
Aqueous solutions for (e) contained either $1.2\times10^{-3}\,mol\,L^{-1}$ benzene or

15 $9.0\times10^{-8}\,mol\,L^{-1}$ anthracene. Ice samples containing benzene were prepared as in (b). Anthracene was deposited onto pure ice surfaces from the gas phase (Kahan and Donaldson, 2007) by flowing dry N_2 at a flow rate of 1 SLPM through a two-necked round bottom flask containing several grams of anthracene, which was immersed in a water bath heated to $\sim50°C$. The saturated nitrogen stream passed through $\sim50\,cm$

20 of PTFE tubing before entering the chamber through a port in the wall. Deposition of anthracene continued for approximately 15 min; anthracene's fluorescence intensity was monitored during deposition to ensure that its surface coverage remained in the non-saturated (i.e. submonolayer) regime (Mmereki and Donaldson, 2003; Kahan and Donaldson, 2007).

25 Hydroxyl radicals were produced from the photolysis of gas-phase HONO. Nitrogen gas was bubbled through a concentrated HCl solution, then passed over glass beads coated with damp $NaNO_2$ (Febo et al., 1995; Aubin and Abbatt, 2007). The HONO thus formed was immediately introduced to the chamber through a port in the wall.

2.3.2 Experimental details

In situ analysis was performed using LIF. The laser used for excitation was either a Nd:YAG-pumped optical parametric oscillator (OPO), which was tunable in the UV between 245 and 355 nm, or a nitrogen laser with emission at 337 nm. Both lasers were operated at 10 Hz. The OPO output pulses were ~4 ns in duration with pulse energies of ~1.5 mJ and the N_2 laser pulses were 3 ns long, with energies of 300 μJ. Emission was collected through a liquid light guide (LLG) oriented perpendicular to the laser beam, and passed through a monochromator, then detected by a photomultiplier tube and sent to a digital oscilloscope for analysis. A 100 ns slice of the fluorescence decay was captured and averaged at each wavelength.

The supplementary information http://www.atmos-chem-phys-discuss.net/9/20881/2009/acpd-9-20881-2009-supplement.pdf displays schematics which show complete details of the experimental conditions in each experiment. For aqueous samples in (b) and (c), the laser beam was oriented horizontally, and the LLG was positioned horizontally to collect emission from the side of the quartz cuvette. All ice samples, as well as aqueous samples in (e), were contained in the reaction chamber. The laser beam entered the chamber such that it impinged upon the sample surface at a very shallow angle (~3° from horizontal) (Kahan and Donaldson, 2007) The LLG was suspended ~1 cm above the sample surface. This geometry affords us surface sensitivity and has allowed us to monitor reactions at air-ice (Kahan and Donaldson, 2007, 2008; Kahan et al., 2007) and air-water (Mmereki and Donaldson, 2003; Clifford et al., 2007) interfaces.

Phenol concentrations in aqueous solution were monitored by exciting samples at 271 nm and monitoring emission at 318 nm, as in the offline experiments. The in situ spectra were identical to those measured offline using the fluorimeter. However, as shown in Fig. 2, the excitation and emission spectra of benzene and phenol at the air-ice interface are quite different from those in aqueous solution, likely due to self-association of benzene and phenol at the air-ice interface (Kahan and Donaldson,

Title Page

Abstract	Introduction
Conclusions	References
Tables	Figures

◄◄	►►
◄	►
Back	Close

Full Screen / Esc

Printer-friendly Version

Interactive Discussion

2007, 2008; Ardura et al., 2009). While the excitation spectra of benzene and phenol overlap on ice, phenol emits in the region between 300 and 320 nm and benzene does not. Therefore, for the experiments in (d) and (e), we monitored phenol formation at the air-ice interface by exciting our ice samples at 261 nm and detecting emission at 318 nm, as indicated by the arrows in the figure. In (e), anthracene loss kinetics at air-water and air-ice interfaces were measured by exciting the samples at 337 nm and monitoring emission at 405 nm (Mmereki and Donaldson, 2003; Kahan and Donaldson, 2007).

In (b), aqueous benzene solutions were contained in 10 mm pathlength quartz cuvettes and were irradiated at room temperature with either the 261 nm output of the OPO, the full output of the 100 W xenon arc lamp, or both. The lamp's output was directed by a first-surface mirror with maximum reflectance at 355 nm onto the sample at a downward angle such that the entire sample was irradiated uniformly. At known time intervals, the laser's output was tuned to 271 nm and phenol's emission intensity was recorded. Ice samples were contained in the reaction chamber, and were irradiated by the 261 nm output of the OPO, by the full output of the 100 W lamp, or by both. The lamp's output was directed by a first-surface mirror onto the sample through a quartz window in the chamber roof. Phenol emission intensity was recorded automatically every 20 s. The distance between the lamp and the samples was ~90 cm for all in situ experiments.

In (c) and (d), samples were irradiated with the output of the 100 W xenon arc lamp which passed through a 295 nm longpass cutoff filter. The lamp geometries were identical to those in (b). For (c), LIF intensity was collected automatically every 20 s. For (d), the laser was blocked during photolysis by the lamp, and the lamp was blocked during data acquisition.

In (e), both aqueous and ice samples were contained in the reaction chamber. Aqueous samples were contained either in a petrie dish or a stainless steel plate with 2 mm high "walls" made of silicone vacuum grease, and ice samples were placed on a stainless steel plate which covered the chamber floor to prevent oxidation of the copper.

Gas-phase HONO was introduced to the chamber and then photolyzed to form OH. This was done either by directing the wavelength-filtered output of the 100 W xenon arc lamp onto the sample surface through the quartz window in the chamber roof, or by introducing the unfiltered output of the lamp into the chamber horizontally through a quartz window in the back of the chamber such that the sample itself was not directly illuminated. LIF measurements of phenol for aqueous and ice samples were performed as in (c) and (d), and LIF measurements of anthracene were performed by exciting the sample with the N_2 laser and measuring emission intensity at 405 nm automatically every 20 s.

2.4 Reagents

All reagents were used as purchased without further purification. Benzene (purity ≥99.0%) and H_2O_2 (lab grade) were purchased from ACP. Anthracene (99% purity) and $NaNO_2$ (Reagent Plus) were from Sigma Aldrich. Nitric acid was from Caledon, and HCl was from Baker. Nitrogen gas (99.998% purity) was from B.O.C. 18 MΩ deionized water was used for all experiments.

3 Results

3.1 Experiment set (a): offline measurements

The aim of this set of experiments was to determine whether the production or reactivity of OH is different at the air-ice interface than it is in liquid pockets within bulk ice and in aqueous solution. We used benzene as an OH trap and measured phenol production rates following the photolysis of H_2O_2 as an OH source in aqueous solution, ice cubes, and ice granules. Full details of the OH-trap are given in the Supplementary Information. Figure 3 shows phenol concentration as a function of irradiation time in the three media. At longer irradiation times, phenol formed in the initial reaction can go on

to react with OH. To avoid this complication, we determined phenol's initial growth rate by the slope of the linear fit to the concentration vs. time data at short irradiation times. The phenol production rates in aqueous solution and in ice cubes were identical within error ($(4.2\pm0.9)\times10^{-10}$ mol L^{-1} s^{-1} and $(4\pm2)\times10^{-10}$ mol L^{-1} s^{-1} respectively). With ice granules, however, no phenol growth was observed. Given the sample volumes and radii, we estimate that the surface area-to-volume ratio of the ice granules is approximately six times greater than that of the ice cubes. This is expected to result in a higher fraction of the reagent existing in the QLL at the surface of the ice granules. Thus we hypothesize that the results from the ice cubes should be more representative of reactivity in liquid pockets within bulk ice, and the results from the ice granules should be more representative of reactivity in the QLL, as we have previously reported (Kahan et al., 2009). The lack of phenol growth in ice granules supports our hypothesis that OH is either produced inefficiently at the air-ice interface, or that it reacts inefficiently with any benzene that is present there.

3.2 Experiment set (b): validation of an in situ OH-probe

To explore whether the results of (a) were due to different behaviour of OH at the air-ice interface compared to in bulk ice and liquid water, we developed an in situ technique to measure phenol formation directly at the air-ice interface. To test this probe's ability to measure phenol growth in real time, we irradiated aqueous and ice samples containing benzene at wavelengths below 295 nm. Under these conditions, benzene should react directly with molecular oxygen to form phenol, as has been observed in the gas phase (Tubaro et al., 2003) and in liquid benzene samples (Stella et al., 2008). Figure 4a shows excitation spectra of an aqueous benzene sample before and after irradiation, as well as an excitation spectrum of phenol. Figure 4b shows emission spectra at an ice surface for a frozen sample containing benzene before and after irradiation. The growth of phenol after irradiation is evident both on ice and in aqueous solution. The presence of phenol in the ice surface experiments was confirmed by acquiring excitation spectra of the melted samples and by HPLC analysis (see the sup-

plementary information for details http://www.atmos-chem-phys-discuss.net/9/20881/ 2009/acpd-9-20881-2009-supplement.pdf). The involvement of O_2(g) in phenol formation was tested by flushing the solutions prior to freezing, as well as the reaction chamber during freezing and irradiation, with N_2. No phenol growth was observed in
5 these conditions, confirming the role of molecular oxygen in the mechanism.

Figure 5 shows the growth in the LIF signal due to phenol formation during irradiation of benzene samples in aqueous solution and at the air-ice interface in the presence of atmospheric O_2. The first-order growth rate is the same in both media. These results show that we are able to monitor the conversion of benzene to phenol in real time both
10 in aqueous solution and at the air-ice interface.

3.3 Experiment set (c): photolysis of OH-precursors in solution

The results of (b) show that the in situ probe is capable of detecting phenol growth in aqueous solution and at the air-ice interface in real time. In (c), we tested the ability of this technique to measure OH formation rates in situ in aqueous solution. We
15 formed OH by irradiating aqueous solutions containing excess benzene and varying concentrations of H_2O_2, HNO_3, or $NaNO_2$ at wavelengths above 295 nm. The photolysis quantum yields and absorption cross sections of these oxidants have been studied both in aqueous solution and in ice (see Chu and Anastasio, 2003, 2005, 2007 and references therein).
20 Figure 6 shows the growth rate of phenol as a function of OH-precursor concentration. At the concentrations used in this work, the dependences are linear, indicating simple second order kinetics, as expected from the rate expression $\frac{d[\text{Ph}]}{dt} = k_{\text{rxn}}$ [OH][B]. Because OH is formed directly from the precursor, we observe linear dependences on the precursor concentration. Using the slope of the linear fits to our
25 data and absorption cross sections and photolysis quantum yields from the literature (Chu and Anastasio, 2003, 2005, 2007), we estimated an approximate average photon flux for our lamp over the wavelengths of absorption of each oxidant (see the supplementary snformation for details http://www.atmos-chem-phys-discuss.net/9/20881/

Hydroxyl radical reactivity at the air-ice interface

T. F. Kahan et al.

Title Page

Abstract	Introduction
Conclusions	References
Tables	Figures

⏮   ⏭

◀   ▶

Back   Close

Full Screen / Esc

Printer-friendly Version

Interactive Discussion

2009/acpd-9-20881-2009-supplement.pdf). In each case, our calculated photon fluxes matched the spectral irradiance of the lamp provided by the manufacturer within a factor of three. The total irradiance of the lamp reaching our sample between 300 and 400 nm is approximately 4×10^{13} photon cm^{-2} s^{-1}, as determined from nitrite photolysis. The good agreement between the predicted spectral irradiance of our lamp and our calculated irradiance based on our measured OH production rates indicates that our in situ probe adequately measures OH production rates.

3.4 Experiment set (d): photolysis of OH-precursors at the air-ice interface

The results of (b) and (c) validated the use of our in situ technique. In (d) we monitored phenol growth at the air-ice interface during the irradiation of frozen samples containing benzene and an OH-precursor. Reagents were either frozen from solution or introduced from the gas phase. Neither reagent concentrations nor sample preparation methods had any effect on the results. Under no experimental conditions did we observe a growth of intensity at 318 nm. This observation offers strong confirmation that the lack of phenol growth observed in the irradiated ice granules (presented in (a), above) was due to differences in reactivity at the air-ice interface compared to in aqueous solution. It is also in agreement with our previous result (Kahan and Donaldson, 2007) that indirect photolysis of anthracene, via OH produced from NO_3^- and H_2O_2, does not occur at the air-ice interface.

3.5 Experiment set (e): heterogeneous reactions at air-water and air-ice interfaces

The results from the previous experiments show that the photolysis of hydroxyl radical precursors in the presence of benzene does not form phenol to an appreciable extent at the air-ice interface. This could be due to one of two reasons: The photochemical production of OH could be suppressed at the air-ice interface compared to in bulk ice and aqueous solution; or hydroxyl radicals could be formed, but not react with ben-

zene. To test the reactivity of hydroxyl radicals toward benzene at the air-ice interface, we formed OH in the gas phase and monitored the heterogeneous reaction between OH and benzene at the surfaces of water and ice. Figure 7 shows the LIF signal intensity associated with phenol growth as a function of the exposure time to HONO(g). During the initial stage of the experiment, when the HONO in the chamber was not irradiated, no growth of phenol was observed on water or on ice. When the lamp was turned on, the HONO photolyzed to form OH, and an immediate growth of phenol was evident at the water surface. However, no growth was observed on ice. We performed this experiment both by irradiating the samples with the filtered ($\lambda > 295$ nm) output of the lamp, and by directing the unfiltered lamp's output just above and parallel to the samples, with no difference in the results.

We also measured the degradation rate of anthracene at air-water and air-ice interfaces due to heterogeneous reaction with OH. To avoid loss of anthracene due to direct photolysis, we irradiated the chamber with the output of the unfiltered lamp oriented such that the sample itself was not illuminated. Figure 8 shows anthracene loss as a function of time during exposure to gas-phase OH. While rapid loss is observed at the air-water interface, no change in anthracene's concentration is observed at the air-ice interface.

These results do not rule out the possibility that hydroxyl radical formation proceeds at a different rate at the air-ice interface than in liquid water or bulk ice. They do, however, clearly show that hydroxyl radicals are much less reactive toward benzene and anthracene at air-ice interfaces than at air-water interfaces, whether the hydroxyl radicals are formed in the QLL through the photolysis of NO_2^-, NO_3^-, or H_2O_2, or introduced from the gas phase.

4   Discussion

As we discuss in (Kahan and Donaldson, 2007), there are several possible explanations for a reduction in reactivity between OH and an organic compound at the air-ice

interface. One possibility is that diffusion rates on the ice surface are lower than those in or on water, leading to slower bimolecular reaction rates. However, we might expect to see a noticeable temperature dependence for the reaction if this were the case; we have not observed a temperature dependence in water or on ice for either the indirect
5 photolysis of anthracene (in the presence of H_2O_2) (Kahan and Donaldson, 2007) or for the heterogeneous ozonation of phenanthrene (Kahan and Donaldson, 2008).

A second possibility is that OH partitions poorly to the ice surface, and is therefore not present in high enough concentrations for us to observe a reaction with benzene, whether the OH is formed in the ice or introduced from the gas phase. We have
10 previously noted (Kahan and Donaldson, 2008) that ozone partitions up to 75% less effectively to an air-ice interface than to a liquid water surface. However, despite its less efficient adsorption, ozone reacted much more quickly with phenanthrene on ice than on liquid water; at 50 ppb ozone, phenanthrene's lifetime toward ozonation would be just under five days on ice, compared to 44 days on water.

15 It is also possible that hydroxyl radicals recombine quickly to form H_2O_2 or their parent compounds. This recombination process is thought to be a major mechanism of H_2O_2 formation in interstellar ices (Pan et al., 2004; Zheng et al., 2006). Although benzene concentrations were in excess of OH by at least an order of magnitude in our samples, it is still possible that OH self-reacted before encountering a benzene
20 molecule. We have previously demonstrated that aromatic compounds self-associate readily at the air-ice interface, even at submonolayer coverages (Kahan and Donaldson, 2007, 2008; Ardura et al., 2009). They likely exist in "islands" scattered across the surface, rather than as a uniform coating. It is possible that the OH is either formed, or adsorbed to the ice surface, in a region that is not populated by benzene. Since the re-
25 combination of OH in ice is thought to occur at close to diffusion-limited rates (Zheng et al., 2006), hydroxyl radicals could recombine before encountering a benzene molecule.

5 Environmental implications

The different reactivities observed at the air-ice interface and in bulk ice suggest that the fate of organics in environmental snow and ice might be quite different depending on whether the compound is frozen from solution (and therefore exists primarily in liquid pockets within the ice) or is deposited from the gas phase (and resides primarily in the QLL). Based on the results of this study, we would expect lifetimes of organic pollutants to be much longer at air-ice interfaces compared to in bulk ice. We have previously seen, however, that direct photolysis rates of PAHs are enhanced at the air-ice interface compared to in liquid water (Kahan and Donaldson, 2007) and bulk ice (Kahan et al., 2009). Heterogeneous ozonation of PAHs is also much faster at air-ice interfaces compared to at air-water interfaces (Kahan and Donaldson, 2008); this reaction is likely unimportant to organic compounds trapped within the ice. Given these observations, we can not draw conclusions about the lifetimes of organic pollutants in snow and ice based on their location. However, we can predict that their fate will be quite different depending on whether they are present at the air-ice interface or in bulk ice, and that in order to properly model their fate, their location must be taken into account.

As a final note, the results of this study emphasize the fact that ice is a complex, heterogeneous, and poorly understood reaction medium. Although treating it as identical to liquid water may be applicable in some cases (i.e. if the reagents are located within the ice bulk), it is clear that this is often not adequate, and may result in large errors in predicted atmospheric lifetimes. We have shown this to be true for aromatic organic compounds, but it is possible that the reactivity of inorganic species is also different at the air-ice interface and in bulk ice. One very important atmospheric reaction is the photochemical formation of OH within snowpacks, which can increase OH mixing ratios in the overlying boundary layer by over an order of magnitude compared to what is expected based on gas-phase processes alone (Domine and Shepson, 2002). While this study and others (Chu and Anastasio, 2003, 2005, 2007) suggest that OH

production rates from the photolysis of inorganic precursors in bulk ice are similar to those in liquid water, it is not certain that the same is true in the QLL. This is important, because snow-air exchange will be most important for OH formed at the air-ice interface. If OH formation rates are different in bulk ice and at the air-ice interface, this will affect our understanding not only of chemistry within snow and ice, but in the overlying atmosphere as well.

References

Anastasio, C. and Chu, L.: Photochemistry of Nitrous Acid (HONO) and Nitrous Acidium Ion (H2ONO+) in Aqueous Solution and Ice, Environ. Sci. Technol., 43, 1108–1114, 2009.

Anastasio, C., Galbavy, E. S., Hutterli, M. A., Burkhart, J. F., and Friel, D. K.: Photoformation of hydroxyl radical on snow grains at Summit, Greenland, Atmos. Environ., 41, 5110–5121, 2007.

Ardura, D., Kahan, T. F., and Donaldson, D. J.: Self-association of naphthalene at the air-ice interface, J. Phys. Chem., 113, 7353–7359, 2009.

Aubin, D. G. and Abbatt, J. P. D.: Interaction of NO2 with hydrocarbon soot: Focus on HONO yield, surface modification, and mechanism, J. Phys. Chem., 111, 6263–6273, 2007.

Carrera, G., Fernandez, P., Vilanova, R. M., and Grimalt, J. O.: Persistent organic pollutants in snow from European high mountain areas, Atmos. Environ., 35, 245–254, 2001.

Chu, L. and Anastasio, C.: Quantum yields of hydroxyl radical and nitrogen dioxide from the photolysis of nitrate on ice, J. Phys. Chem., 107, 9594–9602, 2003.

Chu, L. and Anastasio, C.: Formation of hydroxyl radical from the photolysis of frozen hydrogen peroxide, J. Phys. Chem., 109, 6264–6271, 2005.

Chu, L. and Anastasio, C.: Temperature and wavelength dependence of nitrite photolysis in frozen and aqueous solutions, Environ. Sci. Technol., 41, 3626–3632, 2007.

Hydroxyl radical reactivity at the air-ice interface

T. F. Kahan et al.

Title Page

Abstract	Introduction
Conclusions	References
Tables	Figures

|◀ | ▶|

◀ | ▶

Back | Close

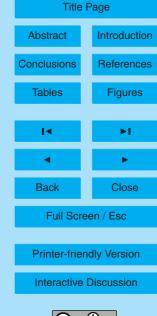Full Screen / Esc

Printer-friendly Version

Interactive Discussion

Cincinelli, A., Stortini, A. M., Checchini, L., Martellini, T., Del Bubba, M., and Lepri, L.: Enrichment of organic pollutants in the sea surface microlayer (SML) at Terra Nova Bay, Antarctica: influence of SML on superfacial snow composition, J. Environ. Monit., 7, 1305–1312, 2005.

Clifford, D., T. Bartels-Rausch and D. J. Donaldson: Suppression of aqueous surface hydrolysis by monolayers of short chain organic amphiphiles, Phys. Chem. Chem. Phys., 2007.

Compoint, M., Toubin, C., Picaud, S., Hoang, P. N. M., and Girardet, C.: Geometry and dynamics of formic and acetic acids adsorbed on ice, Chem. Phys. Lett., 365, 1–7, 2002.

Cotter, E. S. N., Jones, A. E., Wolff, E. W., and Bauguitte, S. J.-B.: What controls photochemical NO and NO_2 production from Antarctic snow? Laboratory investigation assessing the wavelength and temperature dependence, J. Geophys. Res., 108, 8-1–8-10, 2003.

Daly, G. L. and Wania, F.: Organic contaminants in mountains, Environ. Sci. Technol., 39, 385–398, 2005.

Domine, F., Albert, M., Huthwelker, T., Jacobi, H. W., Kokhanovsky, A. A., Lehning, M., Picard, G., and Simpson, W. R.: Snow physics as relevant to snow photochemistry, Atmos. Chem. Phys., 8, 171–208, 2008,
http://www.atmos-chem-phys.net/8/171/2008/.

Domine, F. and Shepson, P. B.: Air-snow interactions and atmospheric chemistry, Science, 297, 1506–1510, 2002.

Dubowski, Y., Colussi, A. J., Boxe, C., and Hoffmann, M. R.: Monotonic increase of nitrite yields in the photolysis of nitrate in ice and water between 238 and 294 K, J. Phys. Chem., 106, 6967–6971, 2002.

Dubowski, Y., Colussi, A. J., and Hoffmann, M. R.: Nitrogen dioxide release in the 302 nm band photolysis of spray-frozen aqueous nitrate solutions. Atmospheric implications, J. Phys. Chem., 105, 4928–4932, 2001.

Dubowski, Y. and Hoffmann, M. R.: Photochemical transformations in ice: Implications for the fate of chemical species, Geophys. Res. Lett., 27, 3321–3324, 2000.

Febo, A., Perrino, C., Gherardi, M., and Sparapani, R.: Evaluation of a High-Purity and High-Stability Continuous Generation System for Nitrous-Acid, Environ. Sci. Technol., 29, 2390–2395, 1995.

Fernandez, P., Carrera, G., Grimalt, J. O., Ventura, M., Camarero, L., Catalan, J., Nickus, U., Thies, H., and Psenner, R.: Factors governing the atmospheric deposition of polycyclic aromatic hydrocarbons to remote areas, Environ. Sci. Technol., 37, 3261–3267, 2003.

Franz, T. P. and Eisenreich, S. J.: Accumulation of polychlorinated biphenyls and polycyclic
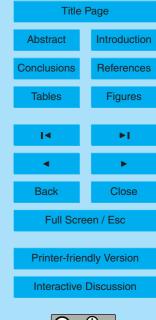
aromatic hydrocarbons in the snowpack of Minnesota and Lake Superior, J. Great Lakes Res., 26, 220–234, 2000.

Galbavy, E. S., Anastasio, C., Lefer, B. L., and Hall, S. R.: Light penetration in the snowpack at Summit, Greenland: Part I – Nitrite and hydrogen peroxide photolysis, Atmos. Environ., 41, 5077–5090, 2007.

Grannas, A. M., Bausch, A. R., and Mahanna, K. M.: Enhanced aqueous photochemical reaction rates after freezing, J. Phys. Chem., 111, 11043–11049, 2007.

Grannas, A. M., Jones, A. E., Dibb, J., Ammann, M., Anastasio, C., Beine, H. J., Bergin, M., Bottenheim, J., Boxe, C. S., Carver, G., Chen, G., Crawford, J. H., Domine, F., Frey, M. M., Guzman, M. I., Heard, D. E., Helmig, D., Hoffmann, M. R., Honrath, R. E., Huey, L. G., Hutterli, M., Jacobi, H. W., Klan, P., Lefer, B., McConnell, J., Plane, J., Sander, R., Savarino, J., Shepson, P. B., Simpson, W. R., Sodeau, J. R., von Glasow, R., Weller, R., Wolff, E. W., and Zhu, T.: An overview of snow photochemistry: evidence, mechanisms and impacts, Atmos. Chem. Phys., 7, 4329–4373, 2007,
http://www.atmos-chem-phys.net/7/4329/2007/.

Herbert, B. M. J., Villa, S., and Halsall, C.: Chemical interactions with snow: Understanding the behavior and fate of semi-volatile organic compounds in snow. Ecotoxicology and Environmental Safety, 63, 3–16, 2006.

Jacobi, H. W., Annor, T., and Quansah, E.: Investigation of the photochemical decomposition of nitrate, hydrogen peroxide, and formaldehyde in artificial snow, J. Photochemi. Photobiol., 179, 330–338, 2006.

Jaffrezo, J. L., Clain, M. P., and Masclet, P.: Polycyclic Aromatic-Hydrocarbons in the Polar Ice of Greenland – Geochemical Use of These Atmospheric Tracers. Atmos. Environ., 28, 1139–1145, 1994.

Kahan, T. F. and D. J. Donaldson: Photolysis of polycyclic aromatic hydrocarbons on water and ice surfaces, J. Phys. Chem., 111, 1277–1285, 2007.

Kahan, T. F. and Donaldson, D. J.: Heterogeneous ozonation kinetics of phenanthrene at the air-ice interface, Environ. Res. Lett., 3, 045006, doi:10.1088/1748-9326/3/4/045006, 2008.

Kahan, T. F., Reid, J. P., and Donaldson, D. J.: Spectroscopic probes of the quasi-liquid layer on ice, J. Phys. Chem., 111, 11006–11012, 2007.

Kahan, T. F., Zhao, R., Jumaa, K. B., and Donaldson, D. J.: Anthracene Photolysis in Aqueous Solution and Ice: Photon Flux Dependence and Comparison of Kinetics in Bulk Ice and at the Air-Ice Interface, Environ. Sci. Technol., submitted, 2009.

Hydroxyl radical reactivity at the air-ice interface

T. F. Kahan et al.

Title Page

Abstract	Introduction
Conclusions	References
Tables	Figures

|◄ | ►|

◄ | ►

Back | Close

Full Screen / Esc

Printer-friendly Version

Interactive Discussion

Klan, P. and Holoubek, I.: Ice (photo)chemistry, Ice as a medium for long-term (photo)chemical transformations – environmental implications. Chemosphere, 46, 1201–1210, 2002.

Klan, P., Klanova, J., Holoubek, I., and Cupr, P.: Photochemical activity of organic compounds in ice induced by sunlight irradiation: The Svalbard project, Geophys. Res. Lett., 30, 46-1–46-4, 2003.

Klanova, J., Klan, P., Heger, D., and Holoubek, I.: Comparison of the effects of UV, H_2O_2/UV and $\gamma\alpha\mu\mu\alpha$-irradiation processes on frozen and liquid water solutions of monochlorophenols, Photochem. Photobiol. Sci., 2, 1023–1031, 2003.

Klanova, J., Klan, P., Nosek, J., and Holoubek, I.: Environmental ice photochemistry: Monochlorophenols, Environ. Sci. Technol., 37, 1568–1574, 2003.

Masclet, P., Hoyau, V., Jaffrezo, J. L., and Cachier, H.: Polycyclic aromatic hydrocarbon deposition on the ice sheet of Greenland. Part I: Superficial snow, Atmos. Environ., 34, 3195–3207, 2000.

Matykiewiczova, N., Kurkova, R., Klanova, J., and Klan, P.: Photochemically induced nitration and hydroxylation of organic aromatic compounds in the presence of nitrate or nitrite in ice, J. Photochem. Photobiol., 187, 24–32, 2007.

Melnikov, S., Carroll, J., Gorshkov, A., Vlasov, S., and Dahle, S.: Snow and ice concentrations of selected persistent pollutants in the Ob-Yenisey River watershed, Sci. Total Environ., 306, 27–37, 2003.

Mmereki, B. T. and Donaldson, D. J.: Direct observation of the kinetics of an atmospherically important reaction at the air-aqueous interface, J. Phys. Chem., 107, 11038–11042, 2003.

Pan, X., Bass, A. D., Jay-Gerin, J.-P., and Sanche, L.: A mechanism for the production of hydrogen peroxide and the hydroperoxyl radical on icy satellites by low-energy electrons, Icarus, 172, 521–525, 2004.

Qiu, R., Green, S. A., Honrath, R. E., Peterson, M. C., Lu, Y., and Dziobak, M.: Measurements of J(NO_3)(-) in snow by nitrate-based actinometry, Atmos. Environ., 36, 2563–2571, 2002.

Ram, K. and Anastasio, C.: Photochemistry of phenanthrene, pyrene, and fluoranthene in ice and snow, Atmos. Environ., 43, 2252–2259, 2009.

Schrimpff, E., Thomas, W., and Herrmann, R.: Regional Patterns of Contaminants (Pah, Pesticides and Trace-Metals) in Snow of Northeast Bavaria and Their Relationship to Human Influence and Orographic Effects, Water Air Soil Poll., 11, 481–497, 1979.

Slater, J. F., Currie, L. A., Dibb, J. E., and Benner, B. A.: Distinguishing the relative contribution of fossil fuel and biomass combustion aerosols deposited at Summit, Greenland through
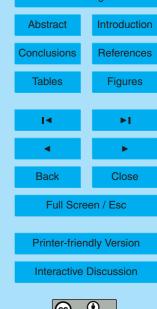
Hydroxyl radical reactivity at the air-ice interface

T. F. Kahan et al.
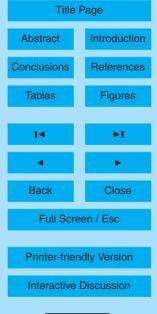
isotopic and molecular characterization of insoluble carbon, Atmos. Environ., 36, 4463–4477, 2002.

Stella, L., Seraglia, R., Sturaro, A., Rella, R., and Traldi, P.: On the photochemical oxidation of benzene and its relevance at environmental level, Rapid Comm, Mass Spectrom,, 22, 257–260, 2008.

Tubaro, M., Marotta, E., Seraglia, R., and Traldi, P.: Atmospheric pressure photoionization mechanisms. 2. The case of benzene and toluene, Rapid Comm. Mass Spectrom., 17, 2423–2429, 2003.

Vione, D., Falletti, G., Maurino, V., Minero, C., Pelizzetti, E., Malandrino, M., Ajassa, R., Olariu, R. I., and Arsene, C.: Sources and sinks of hydroxyl radicals upon irradiation of natural water samples, Environ. Sci. Technol., 40, 3775–3781, 2006.

Wang, X. P., Xu, B. Q., Kang, S. C., Cong, Z. Y., and Yao, T. D.: The historical residue trends of DDT, hexachlorocyclohexanes and polycyclic aromatic hydrocarbons in an ice core from Mt. Everest, central Himalayas, China, Atmos. Environ., 42, 6699–6709, 2008.

Wang, X. P., Yao, T. D., Wang, P. L., Yang, W., and Tian, L. D.: The recent deposition of persistent organic pollutants and mercury to the Dasuopu glacier, Mt. Xixiabangma, central Himalayas, Sci. Total Environ., 394, 134–143, 2008.

Zheng, W., Jewitt, D., and Kaiser, R. I.: Formation of hydrogen, oxygen, and hydrogen peroxide in electron-irradiated crystalline water ice, Astrophys. J., 639, 534–548, 2006.

Hydroxyl radical reactivity at the air-ice interface

T. F. Kahan et al.

Table 1. Excitation and emission wavelengths for spectra in solution and at the air-ice interface.

Sample Description	Spectrum Type	Excitation Wavelength(s) (nm)	Emission Wavelength(s) (nm)
Benzene (solution)	Excitation[a]	245–275	318
	Emission[a]	261	264–472
Benzene (ice)	Excitation[b]	245–315	318
	Emission[b]	261	284–472
Phenol (solution)	Excitation[a]	245–289	318
	Emission[a]	271	264–472
Phenol (ice)	Excitation[b]	245–315	318
	Emission[b]	261	284–472

[a] Spectra were acquired using both LIF (or glancing-angle LIF) and with the commercial fluorimeter.
[b] Spectra were acquired only with LIF (or glancing-angle LIF).

Fig. 1. **(a)** Excitation, and **(b)** emission spectra of aqueous solutions of benzene $(2 \times 10^{-3}\,\text{mol}\,\text{L}^{-1})$ and phenol $(4 \times 10^{-4}\,\text{mol}\,\text{L}^{-1})$ at room temperature. The arrows in (a) and (b) respectively show the excitation and emission wavelengths used to monitor kinetics.

ACPD

9, 20881–20911, 2009
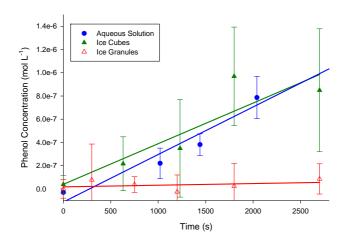
Hydroxyl radical reactivity at the air-ice interface

T. F. Kahan et al.

Title Page

Abstract | Introduction

Conclusions | References

Tables | Figures

|◄ | ►|

◄ | ►

Back | Close

Full Screen / Esc

Printer-friendly Version

Interactive Discussion

Fig. 2. (a) Excitation and (b) emission spectra of frozen aqueous solutions of benzene $(2 \times 10^{-3} \, mol \, L^{-1})$ and phenol $(4 \times 10^{-5} \, mol \, L^{-1})$ acquired at the air-ice interface. The sharp peaks in the emission spectra at ~285 nm are due to Raman scattering from the ice. The arrows in **(a)** and **(b)** respectively show the excitation and emission wavelengths used to monitor kinetics.

Title Page

Abstract | Introduction

Conclusions | References

Tables | Figures

|◄ | ►|

◄ | ►

Back | Close

Full Screen / Esc

Printer-friendly Version

Interactive Discussion

Fig. 3. Phenol concentration as a function of irradiation time for samples containing 1×10^{-3} mol L^{-1} benzene and 9×10^{-4} mol L^{-1} H$_2$O$_2$. The solid traces are linear fits to the data, and error bars represent one standard deviation about the mean for at least three trials.

Printer-friendly Version

Interactive Discussion

Fig. 4. (a) Excitation spectra of a room temperature aqueous solution containing 10^{-3} mol L^{-1} benzene prior to and after irradiation by the 261 nm output of the OPO, as well as an excitation spectrum of phenol in aqueous solution; **(b)** Glancing-angle LIF emission spectra of a frozen solution containing 1×10^{-5} mol L^{-1} benzene prior to and after irradiation by the 261 nm output of the OPO. The sharp peaks around ~285 nm are due to Raman scattering from the ice.

Fig. 5. Growth of phenol fluorescence intensity during irradiation by the full output of the 100 W xenon arc lamp of a 10^{-3} mol L^{-1} benzene in aqueous solution and a frozen 10^{-5} mol L^{-1} benzene solution at the air-ice interface measured at 318 nm. The solid traces are exponential fits to the data.
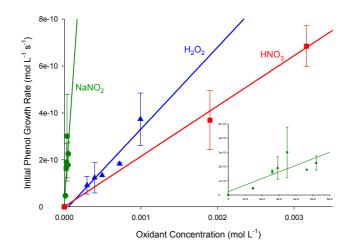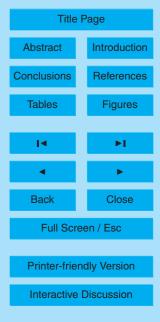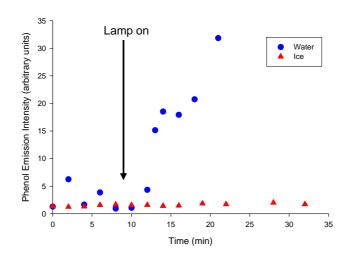
Fig. 6. Initial phenol formation rates as a function of concentration of $NaNO_2$, H_2O_2, and HNO_3 for photolysis in aqueous solutions containing excess benzene. The solid traces are linear fits to the data. Error bars represent one standard deviation about the mean of at least two measurements. An expanded view of phenol's formation rate due to nitrite photolysis is shown in the inset.
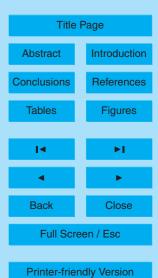
Fig. 7. Phenol fluorescence intensity during the exposure of benzene to gas-phase hydroxyl radicals at air-water and air-ice interfaces. The chamber was flushed with gas-phase HONO, which was irradiated to form OH at $t = 10$ min, as indicated by the arrow.

Fig. 8. Anthracene fluorescence intensity at air-water and air-ice interfaces as a function of exposure time to gas-phase OH. The solid traces are linear fits to the log-normalized data.